



Near-field heat transfer between gold nanoparticle arrays

Anh D. Phan, The-Long Phan, and Lilia M. Woods

Citation: *J. Appl. Phys.* **114**, 214306 (2013); doi: 10.1063/1.4838875

View online: <http://dx.doi.org/10.1063/1.4838875>

View Table of Contents: <http://jap.aip.org/resource/1/JAPIAU/v114/i21>

Published by the [AIP Publishing LLC](#).

Additional information on *J. Appl. Phys.*

Journal Homepage: <http://jap.aip.org/>

Journal Information: http://jap.aip.org/about/about_the_journal

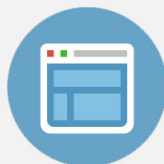
Top downloads: http://jap.aip.org/features/most_downloaded

Information for Authors: <http://jap.aip.org/authors>



Re-register for Table of Content Alerts

Create a profile.



Sign up today!



Near-field heat transfer between gold nanoparticle arrays

Anh D. Phan,^{1,2,a)} The-Long Phan,^{3,b)} and Lilia M. Woods¹

¹Department of Physics, University of South Florida, Tampa, Florida 33620, USA

²Institute of Physics, Vietnam Academy of Science and Technology, 10 Dao Tan, Ba Dinh, Hanoi 10000, Vietnam

³Department of Physics, Chungbuk National University, Cheongju 361-763, South Korea

(Received 14 August 2013; accepted 16 November 2013; published online 4 December 2013)

The radiative heat transfer between gold nanoparticle layers is presented using the coupled dipole method. Gold nanoparticles are modelled as effective electric and magnetic dipoles interacting via electromagnetic fluctuations. The effect of higher-order multipoles is implemented in the expression of electric polarizability to calculate the interactions at short distances. Our findings show that the near-field radiation reduces as the radius of the nanoparticles is increased. Also, the magnetic dipole contribution to the heat exchange becomes more important for larger particles. When one layer is displayed in parallel with respect to the other layer, the near-field heat transfer exhibits oscillatory-like features due to the influence of the individual nanostructures. Further details about the effect of the nanoparticles size are also discussed. © 2013 AIP Publishing LLC. [<http://dx.doi.org/10.1063/1.4838875>]

I. INTRODUCTION

Noble metallic nanoparticles (MNPs) have been exploited in a wide range of technological applications due to their unique properties. In particular, their strong absorption of radiation together with the ability of control of localized surface plasmon resonances have been key factors in a number of optical devices.^{1,2} For many targeted uses and perspectives, periodic two- or three-dimensional MNP arrays have been utilized.^{1,3,4} It was shown that many-body effects⁵⁻⁷ enhance the electromagnetic behavior of the system compared to the one of the individual particles. As two nanoplasmonic arrays are brought at small separations and maintained at different temperatures, radiative heat transfer occurs. The origin of this exchange process originates from the electromagnetic fluctuations between the objects.⁸ Since the electric properties of MNPs are sensitive to the external fields,⁹ it is possible to employ these fields to change the heat radiation. Much experimental¹⁰⁻¹² and theoretical¹³⁻¹⁸ efforts have been devoted in understanding this phenomenon and finding ways for efficient control.

II. THEORETICAL BACKGROUND

In this work, we focus on the radiative heat transfer between two gold MNP layers. Each nanoparticle (NP) is modelled as a dipole. Each layer consists of 20×20 identical particles separated by 1 nm, as shown in Fig. 1. It is assumed that each nanoparticle has a spherical shape with radius R and the dielectric and magnetic properties are described via a dipolar model. The radiative heat exchange $P_{i \rightarrow j}(\omega)$ between the i -th and j -th dipoles consists of electric $P_{i \rightarrow j}^e(\omega)$ and magnetic $P_{i \rightarrow j}^m(\omega)$ contributions,^{19,20} as follows:

$$\begin{aligned} P_{i \rightarrow j}^e(\omega) &= \frac{\omega \epsilon_0}{\pi} \text{Im} \alpha_j^e(\omega) \langle |\mathbf{E}_{ji}|^2 \rangle, \\ P_{i \rightarrow j}^m(\omega) &= \frac{\omega \mu_0}{\pi} \text{Im} \alpha_j^m(\omega) \langle |\mathbf{H}_{ji}|^2 \rangle, \end{aligned} \quad (1)$$

where $\alpha_j^e(\omega)$ and $\alpha_j^m(\omega)$ are the electric and magnetic polarizabilities, respectively, of the j -th dipole with an electric p_j and magnetic m_j components. Also, \mathbf{E}_{ji} and \mathbf{H}_{ji} are the electric and magnetic fields, respectively, at position \mathbf{r}_j due to the fluctuations of dipole. ϵ_0 is the vacuum permittivity and μ_0 is the permeability of free space. The relation between \mathbf{E}_{ji} and the electric dipole moment \mathbf{p}_j is given $\mathbf{E}_{ji}(\omega) = \mu_0 \omega^2 \mathbf{G}(\mathbf{r}_j, \mathbf{r}_i, \omega) \mathbf{p}_j$.^{8,21} Here, $\mathbf{G}(\mathbf{r}_j, \mathbf{r}_i, \omega)$ is the dyadic Green tensor.²¹ Using the fluctuation dissipation theorem,⁸ one finds

$$\begin{aligned} \langle \mathbf{E}_{ji}(\omega) \mathbf{E}_{ji}^*(\omega') \rangle &= \mu_0^2 \omega^2 \omega'^2 \sum_{k,l,t} G_{kl}(\mathbf{r}_j, \mathbf{r}_i, \omega) \\ &\quad \times G_{kt}^\dagger(\mathbf{r}_j, \mathbf{r}_i, \omega') \langle p_{i,l}(\omega) p_{i,t}^*(\omega') \rangle, \\ \langle p_{i,l}(\omega) p_{i,t}^*(\omega') \rangle &= \frac{2\epsilon_0}{\omega} \text{Im} \alpha_i^e(\omega) \Theta(\omega, T_i) \delta_{lt} \delta(\omega - \omega'), \\ \Theta(\omega, T_i) &= \frac{\hbar \omega}{e^{\hbar \omega / k_B T_i} - 1}, \end{aligned} \quad (2)$$

where $k, l, t = x, y, z$; \hbar is the Planck constant, k_B is the Boltzmann constant, and T_i is the temperature of dipole i .

Solving Eqs. (1) and (2) together, the exchanged power caused by the electric dipoles is found to be

$$\begin{aligned} P_{i \rightarrow j}^e(\omega) &= \frac{2 \omega^4}{\pi c^4} \text{Im} \alpha_j^e(\omega) \text{Im} \alpha_i^e(\omega) \Theta(\omega, T_i) \\ &\quad \times \text{Tr}(\mathbf{G}(\mathbf{r}_j, \mathbf{r}_i, \omega) \mathbf{G}(\mathbf{r}_j, \mathbf{r}_i, \omega)^\dagger), \end{aligned} \quad (3)$$

where c is the speed of light.

The approach for the radiative heat transfer assumes that the environment is vacuum with zero temperature. That is why we use the free space Green function \mathbf{G}_0 to construct the dyadic Green function \mathbf{G} between two AuNPs, including the effects of other NPs in the system using the method of

^{a)}Electronic address: anhphan@mail.usf.edu

^{b)}Electronic address: pflong2512@yahoo.com

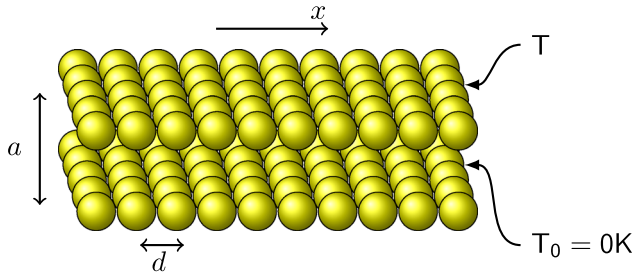


FIG. 1. Schematic representation of two layers of gold MNPs kept at temperature T and 0 K on the top and bottom, respectively. The edge-edge separation distance between two layers is a . The separation between centers of adjacent MNPs is $d = 2R + 1\text{ nm}$.

Ref. 21. Two objects are held at temperature T and 0 at all time and we calculate the dissipated power. There is no heat exchange with the surrounding medium. The influence of the thermal bath, therefore, can be ignored in our calculations.

Similar considerations apply for the magnetic dipole moments and the magnetic fields, yielding $\mathbf{H}_{ji}(\omega) = (\omega/c)^2 \mathbf{G}(\mathbf{r}_j, \mathbf{r}_i, \omega) \mathbf{m}_i$.²² Consequently, the correlation functions for the magnetic dipoles is expressed as¹⁹

$$\langle m_{i,t}(\omega) m_{i,t}^*(\omega') \rangle = \frac{2\delta_{lt}}{\omega\mu_0} \text{Im}\alpha_i^m(\omega) \Theta(\omega, T_i) \delta(\omega - \omega'). \quad (4)$$

Thus, the exchanged power due to the magnetic field fluctuations becomes

$$P_{i \rightarrow j}^m(\omega) = \frac{2\omega^4}{\pi c^4} \text{Im}\alpha_j^m(\omega) \text{Im}\alpha_i^m(\omega) \Theta(\omega, T_i) \times \text{Tr}(\mathbf{G}(\mathbf{r}_j, \mathbf{r}_i, \omega) \mathbf{G}(\mathbf{r}_j, \mathbf{r}_i, \omega)^\dagger). \quad (5)$$

Since particles are taken to be identical, one has $\alpha_1^{e,m} = \alpha_2^{e,m} = \dots = \alpha_N^{e,m} = \alpha^{e,m}$. It is important to note that since the separation distance between two adjacent gold NPs is not much larger than their radius, the influence of higher-order multipoles (quadrupole in our calculation) on the polarizability of MNPs should be taken into account. We can introduce the effective electric and magnetic polarizabilities for MNPs (R less than the skin-depth) derived from the Mie scattering theory^{23,24}

$$\alpha^e(\omega) = 4\pi R^3 \left[\frac{\varepsilon - 1}{\varepsilon + 2} + \frac{1}{12} \left(\frac{\omega R}{c} \right)^2 \frac{\varepsilon - 1}{\varepsilon + 3/2} \right], \quad (6)$$

$$\alpha^m(\omega) = \frac{2\pi}{15} R^3 \left(\frac{\omega R}{c} \right)^2 (\varepsilon - 1),$$

where $\varepsilon(\omega)$ is the dielectric function of gold NPs. The first and second term in the expression of $\alpha^e(\omega)$ correspond to the dipole and quadrupole contributions, respectively. Authors in Ref. 25 used the dipole term and indicated that the distance between centers of MNPs should be at least few times greater than their radius R to ensure the validity of the model for $\alpha^e(\omega)$. It is remarkable that the Mie theory only uses the electric dipole term but well describes the localized surface plasmon resonance (LSPR) of a single NP. The optical property of NP arrays or clusters requires higher-order expansion

of poles.^{23,24} Thus, the quadrupole term added in Eq. (6) allows us to calculate the near-field heat transfer between nanoparticles at shorter distances than calculations from other models^{19,21,25} based on dipole-dipole interactions. For larger NPs ($R \geq 100\text{ nm}$), the expansion in Eq. (6) may not good enough and the higher multipole expansion should be considered.

The heat interchange between two particles is calculated⁸

$$Q_{ij}^{TE, TM}(\omega) = \int_0^\infty d\omega \left[P_{i \rightarrow j}^{e,m}(\omega) - P_{j \rightarrow i}^{e,m}(\omega) \right]. \quad (7)$$

The heat transfer per unit area from the top array to the bottom array is calculated

$$Q = \sum_{i=1}^{N_1} \sum_{j=1}^{N_1+N_1} \left(Q_{ij}^{TE} + Q_{ij}^{TM} \right) / S, \quad (8)$$

where $N_1 = 400$ is the number of NPs in top and bottom object, S is the area of an array, and Q_{TE} and Q_{TM} are the radiative heat transfer of electric and magnetic contribution in NPs, respectively. The first and second sum correspond to the summation of nanoparticles in the bottom layer and the whole system.

III. NUMERICAL RESULTS AND DISCUSSIONS

Increasing the distance d leads to the increase of center-center distance between particles in the systems. The importance of the many-particle effect significantly reduces. Therefore, in our paper, we chose $d = 2R + 1\text{ nm}$ to be suitable with pervious experiments⁴ and clearly exhibit the many-body effects.

The dielectric function of gold NPs is modelled by the Lorentz-Drude (LD) model²⁶

$$\varepsilon(\omega) = 1 - \frac{f_0 \omega_p^2}{\omega(\omega + i\Gamma_0)} + \sum_j \frac{f_j \omega_p^2}{\omega_j^2 - i\omega\Gamma_j - \omega^2}, \quad (9)$$

where f_0 and ω_p are 0.845 and 9.01 eV, respectively. Also, f_j are the oscillator strengths corresponding to characteristic frequencies ω_j and damping parameters Γ_j given in Ref. 26. These parameters were fitted from data set that was measured for gold nanostructure. The first two terms in Eq. (9) describe the contribution of a free electron gas to the response, while the other terms represent interband transitions. In previous studies, authors used the Drude model $\varepsilon(\omega) = 1 - \omega_p^2 / \omega(\omega + i\Gamma_0)$ for the dielectric function of gold. The model is suitable for the dielectric response of bulk, however. The inclusion of the Lorentz oscillators accounts for the localized surface plasmon modes of MNPs with wavelengths $\sim 500\text{ nm}$. Note that the finite spherical size of the nanoparticles affects the damping parameter Γ_0 for gold. Here, we take that $\Gamma_0 \rightarrow \Gamma_0 + A v_f / R$.²⁷ For gold, the parameter $A \approx 1$ and v_f is the Fermi velocity of gold.²⁷

We note that the finite size of the nanoparticles, taken via the modification in Γ_0 , can play an important role in the heat exchange process. Fig. 2 shows a comparison between

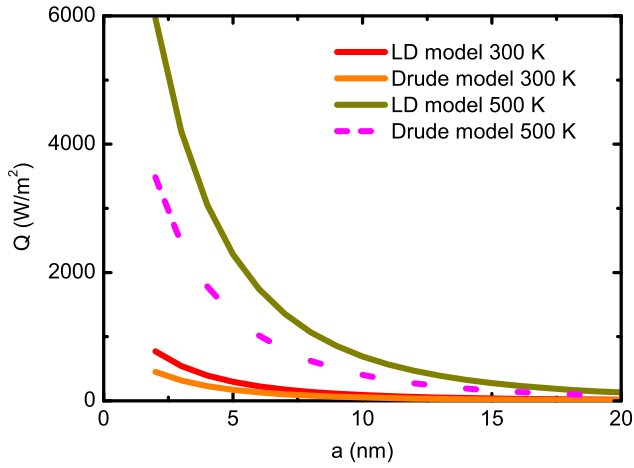


FIG. 2. The radiative heat transfer between two gold MNP layers with $R = 5$ nm as a function of separation distance a at different temperatures T using the Lorentz-Drude and Drude model for the dielectric function.

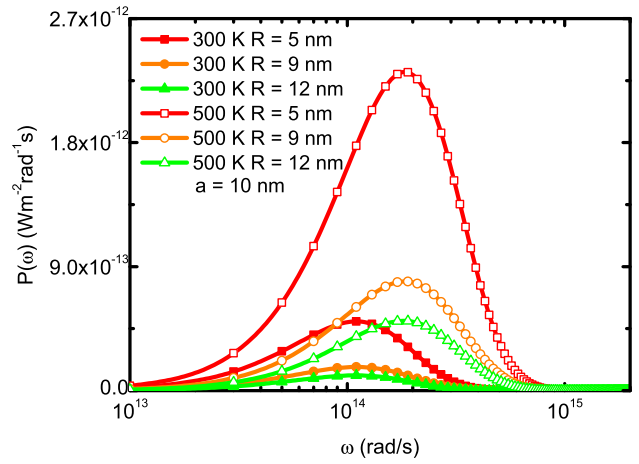


FIG. 3. The heat flux between two gold nanoparticle layers as a function of ω with a variety of R and T at $a = 10$ nm.

the heat transfer between two MNP arrays using the LD and Drude model for $a \geq 2$ nm. The bottom layer is kept at $T_0 = 0$ K, while the top layer is maintained at a finite temperature T .²⁸ For the two chosen temperatures, Q is much larger for the LD model. The huge difference for two models shows that it is impossible to obtain correct value with the Drude model because of the neglect of the bound electron contribution in the polarizability.

To investigate the radiative heat transfer, we have to know the frequency range that is important for the thermal conductance through the heat flux as a function of frequency. The expression of the heat transfer between two arrays versus ω is given

$$P(\omega) = \sum_{s=e,m} \sum_{i=1}^{N_1} \sum_{j=N_1+1}^{N_1+N_1} [P_{i \rightarrow j}^s(\omega) - P_{j \rightarrow i}^s(\omega)], \quad (10)$$

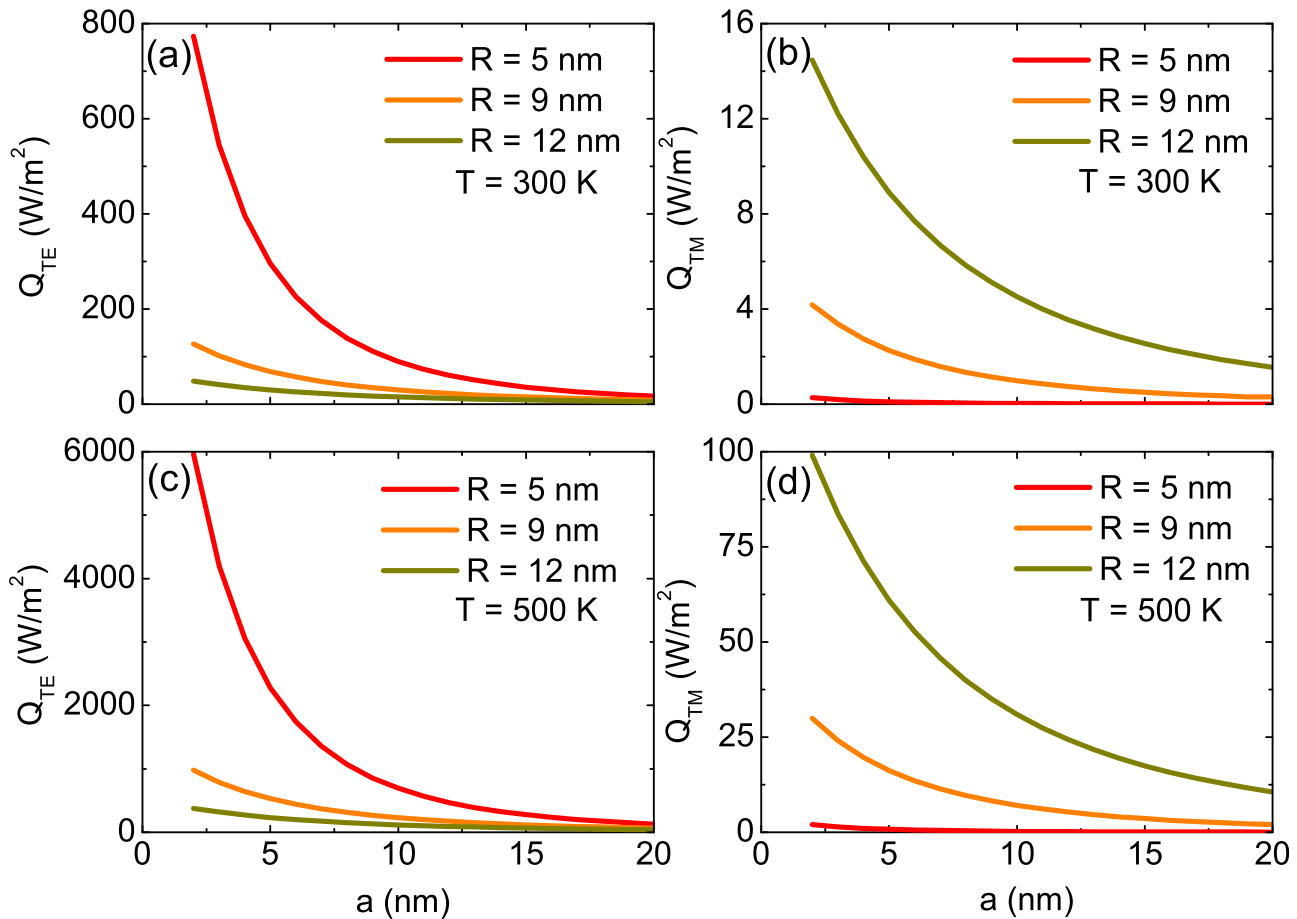


FIG. 4. The heat exchange due to magnetic dipole Q_{TM} and electric dipole Q_{TE} contribution at temperature $T = 300$ and 500 K are calculated for different MNPs with different radii.

where $N_1 = 400$ is the number of nanoparticles in a layer. The first sum corresponds to the two modes (TE and TM), the second one—to the number of particles in the top layer, and the third one—to number of particles in the bottom layer. Figure 3 shows the heat transfer versus frequencies with different sizes of NPs. The radiative heat transfer is contributed significantly by frequencies ranging from 2×10^{13} to 6×10^{14} rad/s. The position of the peak of $P(\omega)$ shifts from left to right when enlarging the nanoparticle's radius.

We also investigate how Q is affected by the TE and TM modes of the system. Fig. 4 shows that for spheres with smaller R , Q_{TE} is dominant. As the radius is increased, the contribution from Q_{TM} becomes more significant. The role of the quadrupole term in the electric polarizability in the absorption and scattering spectrum of MNPs becomes considerable when the NP radius is large²⁴ because of the proportionality of the term to R^5 . The higher-order multipole terms are found to be proportional to $R^{2l+1}/[\epsilon + (l+1)/l]$ with the integer $l \geq 3$. Nevertheless, the quadrupole and higher-order multipole contribution to the heat transfer for the studied structures are small. This is due to the large denominator $[\epsilon + (l+1)/l]$ in the frequency range that is important for the heat transfer $2 \times 10^{13} - 6 \times 10^{14}$ rad/s and small radius R . The contribution of the magnetic polarizability to the heat radiation surpasses that of the quadrupole term. Using Eqs. (3), (5), and (6), one finds that $Q_{TM} \sim R^{10}$ and $Q_{TE} \sim R^6$. Thus, increasing the MNP radius enhances the effect of the magnetic polarizability and reduces the influence of the electric polarizability in the near-field radiation. At certain temperature T and separation distance a , the heat radiation between the two nanoparticles is amplified as R increases. In the layered systems, however, the heat flux Q_{TM} and Q_{TE} dramatically decreases because the distance from a particle to particle located in different layers, except for the nearest neighbors, increases. In comparison with bulk materials, thin film systems with thickness equal to the diameter of the NPs and MNP array systems, the near-field radiation of the nanoparticle arrays is much weaker.²⁹ The main reason is that the layer systems have a small thickness and there is spacing between MNPs. An increase of the MNP radius leads to an increase of empty space in array. The total heat flux Q is found to be 1.92, 1.82, and 1.78 times greater than the heat flux of 400 nearest neighbor pairs of particles placed in two arrays at $a = 2$ nm for $R = 5, 9, 12$ nm, respectively. The ratios decrease when the separation a is expanded since the many-body effects are strengthened if r_{ij}/a is smaller, here, \mathbf{r}_i and \mathbf{r}_j are the positions of particles in different layers, and $\mathbf{r}_{ij} = \mathbf{r}_i - \mathbf{r}_j$.

In Fig. 5, we show results for the heat transfer for the TE and TM modes when there is relative translational displacement along the x axis between the two MNP layers. It is found that the maximum heat is transferred when the layers are completely overlapping ($x = 0$). As the relative displacement between the layers is increased, Q_{TE} and Q_{TM} decrease at an oscillatory-like fashion. One finds that the period of oscillations of 25 nm for the $R = 12$ nm spheres corresponds to distance separation between two neighboring nanoparticles in a layer.

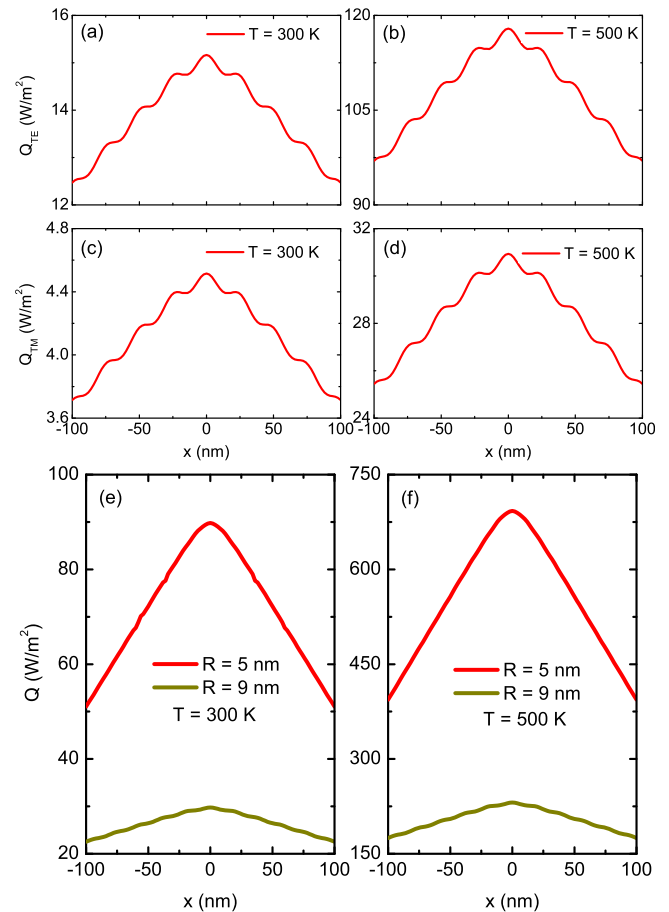


FIG. 5. The radiative heat transfer Q_{TE} and Q_{TM} at $a = 10$ nm as a function of displacement along x axis of the top gold MNP layers with $R = 12$ nm shown in (a)–(d) at 300 and 500 K. The net heat flux versus x with $R = 5$ and 9 nm described in (e) and (f), respectively, at 300 and 500 K.

Combining the contributions from both modes, it is found that the oscillatory-like behavior of Q vs x is not as pronounced, although some oscillations are seen for the nanoparticles with radius $R = 9$ nm (Figs. 5(e) and 5(f)). Our calculations indicate that the heat transfer depends strongly on the overlap between the two layers when sliding one array along x axis with respect to each other. The oscillatory trends of Q_{TE} and Q_{TM} for NPs $R = 12$ nm are observed by means of the couple dipole method in Figs. 5(a)–5(d). It is very easily to see that the period of this oscillatory behavior between two neighboring peaks is approximately 25 nm, which relatively corresponds to the distance d between two nearest NPs at the same array. It suggests that the oscillatory feature depends on how well the horizontal plane projections of the top gold NP array and the bottom one matches each other. For $R = 9$ nm, Figs. 5(c) and 5(d) still show the periodic oscillation in the heat transfer band although this behavior is quite small. Thus, one can conclude that when $a \gg R$, the actual distribution of the nanoparticles is not important, however, the overlap between the layers can change Q by several orders of magnitude.

IV. CONCLUSIONS

This paper has presented theoretical calculations for the near-field radiation in systems involving gold MNPs. Our

method can investigate the discrete nanostructures with arbitrary geometries and consider the size effect of NPs including in the dielectric response. We have considered the role of the structure of MNP layers on the heat transfer when these two arrays are displaced with respect to each other along parallel and perpendicular directions. These results can provide guidelines for designing thermal devices utilizing electromagnetic radiation.

ACKNOWLEDGMENTS

Lilia M. Woods acknowledges the Department of Energy under Contract DE-FG02-06ER46297.

¹B. Auguie and W. L. Barnes, *Phys. Rev. Lett.* **101**, 143902 (2008).

²S. K. Ghosh and T. Pal, *Chem. Rev.* **107**, 4797 (2007).

³Y. Chu, E. Schonbrun, T. Yang, and K. B. Crozier, *Appl. Phys. Lett.* **93**, 181108 (2008).

⁴J. Herrmann, K.-H. Muller, T. Reda, G. R. Baxter, B. Raguse, G. J. J. B. de Groot, R. Chai, M. Roberts, and L. Wiczorek, *Appl. Phys. Lett.* **91**, 183105 (2007).

⁵V. Yannopapas and N. V. Vitanov, *Phys. Rev. Lett.* **110**, 044302 (2013).

⁶V. Yannopapas, *J. Phys. Chem. C* **117**, 14183 (2013).

⁷P. Ben-Abdallah, K. Joulain, J. Drevillon, and C. L. Goff, *Phys. Rev. B* **77**, 075417 (2008).

⁸K. Joulain, "Radiative transfer on short length scales" in *Microscale and Nanoscale Heat Transfer, Topics in Applied Physics* (Springer, Berlin, 2007), Vol. 107, Chap. XVI.

⁹G. M. Wysin, V. Chikan, N. Young, and R. K. Dani, *J. Phys.: Condens. Matter* **25**, 325302 (2013); e-print [arXiv:cond-mat.mes-hall/1305.1252](http://arxiv.org/abs/cond-mat.mes-hall/1305.1252).

¹⁰P. J. van Zwol, L. Ranno, and J. Chevrier, *Phys. Rev. Lett.* **108**, 234301 (2012).

¹¹B. Guha, C. Otey, C. B. Poitras, S. Fan, and M. Lipson, *Nano Lett.* **12**, 4546 (2012).

¹²E. Rousseau, A. Siria, G. Jourdan, S. Volz, F. Comin, J. Chevrier, and J.-J. Greffet, *Nat. Photonics* **3**, 514 (2009).

¹³E. Rousseau, M. Laroche, and J.-J. Greffet, *Appl. Phys. Lett.* **95**, 231913 (2009).

¹⁴E. Rousseau, M. Laroche, and J.-J. Greffet, *J. Appl. Phys.* **111**, 014311 (2012).

¹⁵A. I. Volokitin and B. N. J. Persson, *Phys. Rev. B* **63**, 205404 (2001).

¹⁶V. Yannopapas, *Phys. Rev. B* **73**, 113108 (2006).

¹⁷V. Yannopapas and N. V. Vitanov, *Phys. Rev. B* **80**, 035410 (2009).

¹⁸A. Manjavacas and F. J. G. de Abajo, *Phys. Rev. B* **86**, 075466 (2012).

¹⁹P.-O. Chapuis, M. Laroche, S. Volz, and J.-J. Greffet, *Appl. Phys. Lett.* **92**, 201906 (2008).

²⁰P.-O. Chapuis, M. Laroche, S. Volz, and J.-J. Greffet, *Phys. Rev. B* **77**, 125402 (2008).

²¹P. Ben-Abdallah, S.-A. Biehs, and K. Joulain, *Phys. Rev. Lett.* **107**, 114301 (2011).

²²J. D. Jackson, *Classical Electrodynamics*, 3rd ed. (Wiley, New York, 1998).

²³M. Quinten, *Optical Properties of Nanoparticle Systems* (Wiley, Germany, 2011).

²⁴K. L. Kelly, E. Coronado, L. L. Zhao, and G. C. Schatz, *J. Phys. Chem. B* **107**, 668 (2003).

²⁵G. Domingues, S. Volz, K. Joulain, and J.-J. Greffet, *Phys. Rev. Lett.* **94**, 085901 (2005).

²⁶A. D. Rakic, A. B. Djuric, J. M. Elazar, and M. L. Majewski, *Appl. Opt.* **37**, 5271 (1998).

²⁷V. Amendola and M. Meneghetti, *J. Phys. Chem. C* **113**, 4277 (2009).

²⁸S. Shen, A. Mavrokefalos, P. Sambegoro, and G. Chen, *Appl. Phys. Lett.* **100**, 233114 (2012).

²⁹See Supplemental material at <http://dx.doi.org/10.1063/1.4838875> for information regarding how the near-field heat transfer between two gold thin films held at 0 K and 300 K are calculated.